Percolation threshold and permeability of crystallizing igneous rocks: The importance of textural equilibrium

M.J. Cheadle Department of Geology and Geophysics, University of Wyoming, Laramie, Wyoming 82071, USA
M.T. Elliott British Petroleum Exploration (Angola) Ltd., Compass Point, Staines, Middlesex TW18 1DY, UK
D. McKenzie Department of Earth Sciences, Bullard Laboratories, Madingley Road, University of Cambridge, Cambridge CB3 0EZ, UK

ABSTRACT

The permeability of a crystal mush fundamentally controls the ability of its melt to migrate or segregate with respect to the solid phase and thus controls the extent to which compaction and porous-media convection can occur in crystallizing igneous cumulates. In particular, the existence of a percolation threshold, which defines the porosity at which a crystallizing rock becomes impermeable, can limit the effectiveness of these processes. We present three-dimensional numerical models of the topology of porosity in both texturally equilibrated and nonequilibrated crystal-melt systems; these models enable porosity vs. permeability relationships and hence percolation thresholds to be calculated. The permeability of the nonequilibrated models was calculated using a network-simulation method. These models confirm that there is no percolation threshold for a perfectly texturally equilibrated rock with dihedral angles of <60°. Conversely, the models indicate that the percolation threshold for non–texturally equilibrated rocks is 8%–11%. The models show that permeability is only weakly dependent on the morphology of the crystals at porosities of >20%. These results suggest that the volume of trapped melt in an igneous cumulate may be controlled by the ability of the crystallizing crystal-melt system to reach textural equilibrium.

Keywords: percolation threshold, permeability, cumulates, textural equilibrium, trapped melt.

INTRODUCTION

The gravitationally driven movement of melt with respect to crystallizing solids is a fundamental process that occurs within igneous intrusions. This movement takes place during compaction (McKenzie, 1984) and/or porous-media convection (Tait and Jaupart, 1992), and leads to the generation of igneous cumulates, essential components of all magma chambers. The efficiency of both of these processes is partly controlled by the permeability of the crystallizing cumulates, which in turn depends on the volume, connectivity, and topology of the porosity. The porosity topology is determined by the growth and grain size of the crystals that compose the cumulate. There are two end-member cases: crystal growth with concomitant textural equilibration and crystal growth without textural equilibration. Here we present numerical models of the porosity of crystallizing igneous rocks with and without textural equilibration and use these models to calculate the evolution of the permeability during crystallization. The existence of so-called percolation thresholds, defined as the porosity at which rocks become impermeable, is of particular interest. If a percolation threshold is reached during crystallization, porous-media convection and compaction will both cease, and a trapped melt (e.g., Irvine, 1980; Bedard, 1994) will be retained within the igneous cumulate. The possible development of single-phase cumulates, such as pure anorthosites and dunites, within an intrusion will be limited if the crystal-melt systems exhibit a high-porosity percolation threshold.

PERMEABILITY OF TEXTURALLY EQUILIBRATED ROCKS

Textural, or microstructural, equilibrium occurs when the surface of the solid phase is in chemical equilibrium with the fluid phase and when interfacial-energy–driven equilibration of the fluid-solid interfaces can occur faster than the change in shape or volume of the pore due to crystal growth or deformation. Smith (1948) and Beeré (1975) pioneered the concept and Bulau et al. (1979), von Bargen and Waff (1986), Hunter (1987), and Wark and Watson (1998), among others, applied the concept to the field of geology. If a rock is texturally equilibrated, the topology of the fluid-filled pores will be controlled by the relative interfacial energies of crystal-crystal and crystal-melt contacts. The ratio of these two interfacial energies determines the angle formed between the two walls of a pore at the crystal-crystal-melt junction; this angle is called the dihedral angle (Smith, 1948). It is this angle and the requirement that crystal-melt interfaces be minimum-energy surfaces that determine pore topology in texturally equilibrated rocks. Complications arise because most rocks have variable grain size, consist of more than one phase, and the various phases are likely to be anisotropic with respect to surface energy (e.g., Cooper and Kohlstedt, 1982; Waff and Faul, 1992; Faul, 1997). These properties require that dihedral angles vary throughout the rock, that pore walls may be flat or faceted, and that melt distribution will be somewhat irregular. Static recrystallization can also generate transient disequilibrium melt distributions (Walte et al., 2003). However, Smith (1964), Bulau et al. (1979), Watson (1982), and Faul (2000) showed that as long as the dihedral angles are <60°, the melt phase will form an interconnected network throughout the entire rock to vanishingly small porosities irrespective of these complications. Melt interconnection is the critical property, which characterizes texturally equilibrated melt-bearing rocks.

Beeré (1975), von Bargen and Waff (1986), and Cheadle (1989) applied the theory of textural equilibrium to determine the three-dimensional pore topology of texturally equilibrated rocks and materials. To make the problem tractable, they assumed a monomineralic solid, with constant grain size and isotropic surface energies. Examples of the calculated pore topologies are shown in Figure 1. These models do not predict the faceting of pore faces or the complex melt topologies shown in texturally equilibrated partial melt experiments (Waff and Faul, 1992). However, they are useful because (1) they produce interconnected melt networks typical of texturally equilibrated rocks and (2) they mimic the rounded crystal faces often preserved in igneous cumulates (see Hunter, 1987). Rounded crystal faces exist, because above the roughening temperature, near the melting point of the crystalline phase, crystal faces can more easily assume whatever curvature is needed to accommodate melt (Waff and Faul, 1992). Von Bargen and Waff (1986) used their model to determine porosity vs. permeability relationships for porosities ranging from 0.5% to 5.0% and dihedral angles ranging from 20° to 75°. Cheadle (1989) developed a similar model and extended the range of calculated porosity vs. permeability relationships from 0.1% to 46% porosity, and all dihedral angles (0°–180°), and showed that the porosity vs. per-

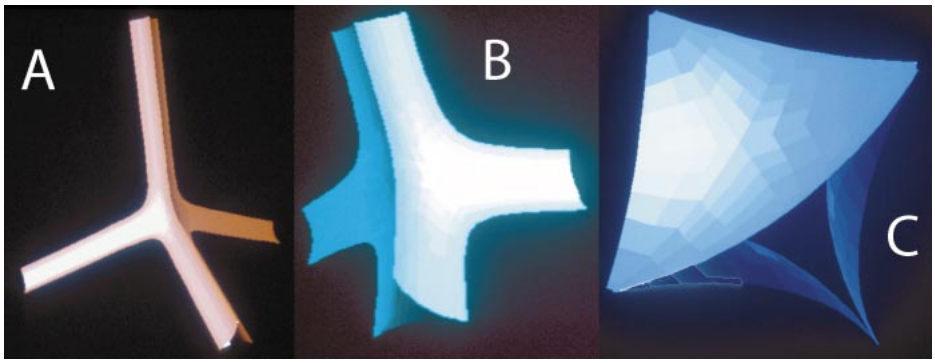

Figure 1. Examples of topologies of texturally equilibrated pore space in monomineralic rock with uniform grain size and isotropic surface energies. Each picture illustrates tetrahedrally symmetric corner unit of porosity, which would reside where four crystals meet. A: Dihedral angle = 1°, porosity = 0.1%. B: Dihedral angle = 1°, porosity = 1.01%. C: Dihedral angle = 1°, porosity = 35%.

meability relationships for dihedral angles from 0° to 40° are very similar. Both papers used an analytical solution for the permeability of connected cylindrical channels residing along the edges of crystals (Frank, 1968), and a geometrical correction was applied to account for the different topology of the porosity of their models. Wark and Watson (1998) (their Fig. 2) showed that the porosity vs. permeability relationships developed by these authors are similar and compared them to permeability measurements on synthetic monomineralic aggregates of quartz and calcite. Liang et al. (2001) refined these measurements to account for the Klinkenberg (slip) effect and produced an empirical porosity vs. permeability relationship that predicts a permeability only 5–10 times lower than that predicted by the numerical permeability relationships of von Bargen and Waff (1986) and Cheadle (1989). Wark et al. (2003) suggested that the lower permeability of the empirical measurements is a consequence of the simplifying assumptions of constant grain size and isotropic surface energy in the numerical models, a result that implies that the effect of pore-wall faceting is comparatively small.

Both theoretical and experimental studies on natural aggregates suggest that texturally equilibrated melt-crystal systems with dihedral angles of $<60°$ will be permeable at porosities as low as 0.5%. Consequently there is a very small effective percolation threshold for texturally equilibrated rocks with dihedral angles of $<60°$, and monomineralic igneous cumulates may be formed under these conditions with extremely low proportions ($<0.5\%$) of trapped melt. This result implies that monomineralic igneous cumulates are most likely to form in larger, slower cooling magma chambers, where textural equilibrium can keep pace with crystal growth.

PERMEABILITY OF TEXTURALLY NONEQUILIBRATED ROCKS

Elliott (1998) developed a computer algorithm capable of simulating the three-dimensional crystallization of simplified melt-crystal systems without textural equilibration. This algorithm allows crystals to be nucleated in a predefined spatial pattern and temporal order within a three-dimensional volume. The crystals are then allowed to grow by the accretion of additional layers to the surface of each crystal in order to simulate crystallization. Complicated, realistic rock textures are produced by the impingement and interference of the growing crystals (Fig. 2). Variations in nucleation density, anisotropic growth rates, and the relative timing of phase nucleation permit the simulation of different textures (Elliott et al., 1997). We present here two simple models of a crystal-melt system. The first—termed the random-cube model—consists of crystallizing randomly oriented and distributed cube-shaped crystals. The second—termed the settled-cube model—consists of crystallizing randomly oriented cube-shaped crystals that have a dense random packing equivalent to that experimentally determined for spheres (Finney, 1970). The latter model simulates the crystallization of an igneous cumulate in which a touching framework of crystals is generated by gravitational settling. These models enable the characterization of the three-dimensional topology and interconnectedness of the evolving porosity as the simulated rock crystallizes and thus permit the permeability of a texturally nonequilibrated crystal-melt system to be calculated.

The determination of the topology of the porosity in the model is nontrivial. The porosity has to be partitioned into a network of individual pores connected at pore throats to enable a network simulation to be used to calculate the permeability of the model (see Bryant and Blunt, 1992). This procedure requires the determination of the location of the centers of individual pores, the number of pores to which each pore is connected, and the shape and cross-sectional area of the pore throats perpendicular to a line joining each pair of connected pores. Elliott (1998) developed a method to do this similar to that of Baldwin et al. (1996). An iterative three-dimensional porosity-erosion method called morphological thinning (Lin and Cohen, 1982; Thovert et al., 1993; Spanne et al., 1994) is used to determine the location of the center of each pore and to subdivide the porosity into individual pores. The centers of individual pores are then numerically regrown by dilation to mimic the topology of the original porosity. The pore throats are defined by where the individual pores meet (Fig. 3A). Once the topology and the centers of the individual pores are known, the separation of interconnected pores and the size of the pore throats can be easily calculated. (For further details, see Elliott, 1998.)

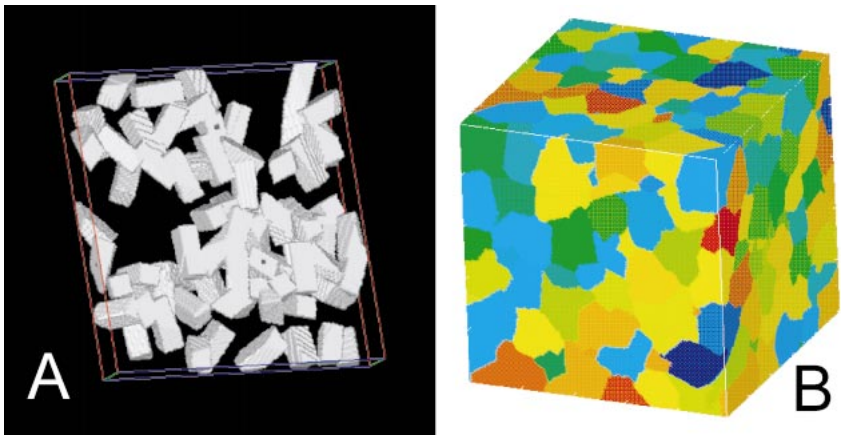

Figure 2. A: Slice through computer-generated volume showing three-dimensional topology of partially crystallized monomineralic rock. Individual crystals are rectangular prisms with 3:1:1 aspect ratio. B: Larger computer-generated volume showing fully crystallized synthetic rock: 395 randomly oriented cube-shaped crystals were allowed to grow and impinge on one another until all pore space was filled.

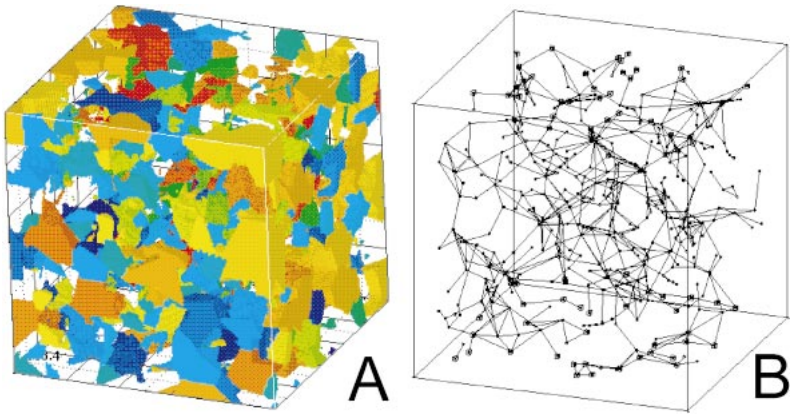

Figure 3. A: Computer-generated porosity model. In this model, pores, not solid matrix, are illustrated. Each pore is colored differently. Crystals (n = 900) forming solid matrix are not shown, and so this model is inverse to model similar to that of Figure 2A. B: Three-dimensional network model for porosity model shown in A. Small dots represent pore centers (nodes) in network, and large cubes represent centers of pores that are connected to either upper or lower faces of volume.

Permeability of the models can be calculated by using a network-simulation method (e.g., Doyen, 1988; Bryant and Blunt, 1992) because the topology of the porosity is completely defined (Elliott, 1998). The topology of the network used for calculating the permeability was extracted from the partitioned porosity. Figure 3B shows an example of such a network. Lines connecting pore centers represent flow paths within the model. Some of the flow paths terminate within the model volume; these are known as dead-end branches, and they do not contribute to the permeability of the system and therefore were removed from the calculations (Elliott, 1998). In order to calculate the permeability, the hydraulic conductivity of the connected individual flow paths was determined by using the parameters derived from the pore-space characterization (the path length or separation between pore centers and the pore throat area or radius). The product of the hydraulic conductivity and the pressure drop along a flow path gives the flow rate through the path. Once the conductivities were calculated, a pressure gradient was imposed across the network to find the steady-state pressures in the network sites. The permeability derives from the calculated net flow rate through the network at the imposed steady-state pressure gradient.

The algorithms were tested by calculating the permeability of an example of the Fontainebleau sandstone, with a known, experimentally determined permeability (1.3 μm^2, Schwartz et al., 1994). A three-dimensional X-ray tomographic image of this sample (Coker et al., 1996) was provided by David Coker. Our algorithms were used to characterize the pore space of this sample and to calculate its permeability. We obtained values of 1.1 and 1.4 μm^2 for the permeability along the two long directions of the sample, which are in good agreement with the experimentally measured permeability.

Permeability-porosity relationships are presented for the random-cube model and the settled-cube model (Fig. 4). They were determined for cubic volumes consisting of ~900 crystals. Three different permeability calculations, corresponding to the mutually perpendicular axes of the cube, were made at each (5%) increment of crystallization, starting at 33% porosity and decreasing to 8% porosity, below which the permeability had decreased to zero. In all cases, the three permeabilities were similar, and their average was used as the calculated permeability. The crystallization step size was constrained by the minimum width of the growth increment on the crystals, which in turn was constrained by the size of the models and available computer processing time.

The major result of these calculations is that the permeability of both of the models drops to zero between 8% and 11% porosity, suggesting that non–texturally equilibrated melt-crystal systems may have percolation thresholds as high as 8%–11% porosity. This is the fundamental difference from texturally equilibrated systems, which have much lower percolation thresholds. Igneous cumulates formed under conditions that are not conducive to textural equilibrium may therefore contain a minimum of 8%–10% trapped melt.

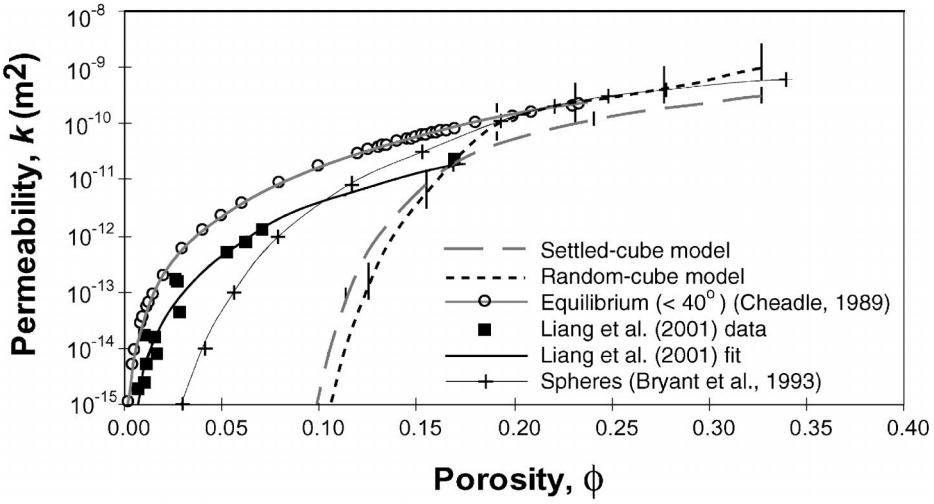

Figure 4. Permeability vs. porosity plot showing various porosity vs. permeability relationships discussed in this paper. Data are scaled for crystal grain size of 1 mm.

DISCUSSION

Figure 4 shows the calculated porosity vs. permeability relationships for the models presented in this paper together with the calculated relationship for the overgrowth of a dense random packing of touching spheres (Bryant et al., 1993), which successfully models the porosity vs. permeability relationships of the Fontainebleau sandstone (Bourbie and Zinszner, 1985), and the experimental porosity vs. permeability data of Liang et al. (2001). In each case, the data are scaled to show the permeability of a crystal-melt system with 1-mm-diameter crystals. The porosity vs. permeability curve for a texturally equilibrated rock is for a dihedral angle of 1°. This particular dihedral angle was chosen for two reasons: (1) Its corresponding porosity vs. permeability relationship is representative of the relationships for all dihedral angles up to 40°. (2) It allows the permeability determinations to be corrected for calculation errors at high porosities (Cheadle, 1989), because at the porosity of disaggregation, the topology of the porosity must be that of close-packed touching spheres (Fig. 1C), and thus the predicted permeability must be similar to that measured experimen-

tally for densely packed touching spheres (Bryant and Blunt, 1992).

At porosities of >20%, all the porosity vs. permeability relationships are similar to within half an order of magnitude permeability. This result suggests that permeability of crystallizing systems at porosities of >20% is largely independent of crystal shape (cubic vs. spherical vs. ideally texturally equilibrated), presumably because the porosity channels are relatively large and open in all cases. At porosities below 20%, channel blocking begins (Bryant et al., 1993), and permeabilities are shown to be very dependent on the shape of the crystals in the crystal-melt system and thus the degree to which the system is texturally equilibrated. Further, percolation thresholds vary from <0.5% porosity for crystallizing systems composed of perfectly texturally equilibrated crystals (for dihedral angles <60°), through 3% porosity for crystallizing systems composed of nonequilibrated spherically shaped crystals, to ~10% porosity for crystallizing systems composed of nonequilibrated cube-shaped crystals. The percolation threshold is largest for crystallizing systems composed of cube-shaped crystals. This is because a cube has a greater maximum length than a sphere of similar volume and therefore a greater chance of contact with a neighboring crystal, leading to it being more likely to block porosity channels in the rock. It is interesting to note that the random-cube model appears to have a slightly higher percolation threshold than the settled-cube model. This is a consequence of the larger grain-size variation inherent in the random-cube model. Nonequilibrated crystal-melt systems consisting of more realistically shaped crystals will likely have percolation thresholds between those calculated for spherical and cubic crystals. These results imply that the final 5%–10% of melt in a crystallizing magma cannot be extracted unless the rock is texturally equilibrated. This effect may explain the commonly found occurrence of ~5%–10% trapped melt in some igneous cumulates.

ACKNOWLEDGMENTS

We thank Steve Bryant for being a permeability guru from afar, David Coker for providing the Fontainebleau sandstone tomographic image, Dougal Jerram and Dave Wark for constructive reviews, Barbara John for editorial help, and the Natural Environment Research Council (NERC) for studentships for Cheadle and Elliott.

REFERENCES CITED

Baldwin, C., Sederman, A.J., Mantle, M.D., Alexander, P., and Gladden, L.F., 1996, Determination and characterization of the structure of a pore space from 3D volume images: Journal of Colloid and Interface Science, v. 181, p. 79–92.

Bedard, J.H., 1994, A procedure for calculating the equilibrium distribution of trace elements among the minerals of cumulate rocks and the concentration of trace elements in the coexisting liquids: Chemical Geology, v. 118, p. 143–153.

Beeré, W., 1975, A unifying theory of the stability of penetrating liquid phases and sintering pores: Acta Metallurgica, v. 23, p. 131–138.

Bourbie, T., and Zinszner, B., 1985, Hydraulic and acoustic properties as a function of porosity in Fontainebleau sandstone: Journal of Geophysical Research, v. 90, p. 11,525–11,532.

Bryant, S., and Blunt, M., 1992, Prediction of relative permeability in simple porous media: Physical Review A, v. 46, p. 2004–2011.

Bryant, S., Cade, C., and Mellor, D., 1993, Permeability prediction from geologic models: American Association of Petroleum Geologists Bulletin, v. 77, p. 1338–1350.

Bulau, J.R., Waff, H.S., and Tyburczy, J.A., 1979, Mechanical and thermodynamic constraints on fluid distributions in partial melts: Journal of Geophysical Research, v. 84, p. 6102–6108.

Cheadle, M.J., 1989, Properties of texturally equilibrated two-phase aggregates [Ph.D. thesis]: Cambridge, University of Cambridge, 163 p.

Coker, D.A., Torquato, S., and Dunsmuir, J.H., 1996, Morphology and physical properties of Fontainebleau sandstone via a tomographic analysis: Journal of Geophysical Research, v. 101, p. 17,497–17,506.

Cooper, R.F., and Kohlstedt, D.L., 1982, Interfacial energies in the olivine-basalt system, *in* Akimoto, S., and Manghani, M.H., eds., High pressure research in geophysics: Advances in earth and planetary sciences: Tokyo, Japan, Center for Academic Publications, v. 12, p. 217–228.

Doyen, P.M., 1988, Permeability, conductivity and pore geometry of sandstone: Journal of Geophysical Research, v. 93, p. 7729–7740.

Elliott, M.T., 1998, The three-dimensional numerical simulation of crystallizing media [Ph.D. thesis]: Liverpool, University of Liverpool, 73 p.

Elliott, M.T., Cheadle, M.J., and Jerram, D.A., 1997, On the identification of textural equilibrium in rocks using dihedral angle measurements: Geology, v. 25, p. 355–358.

Faul, U.H., 1997, Permeability of partially molten upper mantle rocks from experiments and percolation theory: Journal of Geophysical Research, v. 102, p. 10,299–10,311.

Faul, U.H., 2000, Constraints on the melt distribution in anisotropic polycrystalline aggregates undergoing grain growth, *in* Bagdassarov, N., et al., eds., Physics and chemistry of partially molten rocks: Norwell, Massachusetts, Kluwer Academic Publishers, p. 67–92.

Finney, J.L., 1970, The geometry of random packing: Royal Society of London Proceedings, ser. A, v. 319, p. 479–493.

Frank, C.F., 1968, Two-component flow model for convection in the Earth's upper mantle: Nature, v. 220, p. 350–352.

Hunter, R.H., 1987, Textural equilibrium in layered igneous rocks, *in* Parsons, I., ed., Origins of igneous layering: Boston, Massachusetts, D. Reidel Publishing Company, p. 473–503.

Irvine, T.N., 1980, Magmatic infiltration metasomatism, double-diffusive fractional crystallization, and adcumulus growth in the Muskox intrusion and other layered intrusions, *in* Hargraves, R.B., ed., Physics of magmatic processes: Princeton, New Jersey, Princeton University Press, p. 325–384.

Liang, Y., Price, J.D., Wark, D.A., and Watson, E.B., 2001, Nonlinear pressure diffusion in a porous medium: Approximate solutions with applications to permeability measurements using transient pulse decay method: Journal of Geophysical Research, v. 106, p. 529–535.

Lin, C., and Cohen, M.H., 1982, Quantitative methods for geometric modeling: Journal of Applied Physics, v. 53, p. 4152–4165.

McKenzie, D.P., 1984, The generation and compaction of partially molten rock: Journal of Petrology, v. 25, p. 713–765.

Schwartz, L.M., Auzerias, F., Dunsmuir, J., Martys, N., Bentz, D.P., and Torquato, S., 1994, Transport and diffusion in three-dimensional composite media: Physica A, v. 207, p. 28–36.

Smith, C.S., 1948, Grain phases and interfaces: An interpretation of microstructure: American Institute of Mechanical Engineers Transactions, v. 75, p. 15–51.

Smith, C.S., 1964, Some elementary principles of polycrystalline microstructure: Metallurgical Review, v. 9, p. 1–48.

Spanne, C.S., Thovert, J.F., Jacquin, C.J., Lindquist, W.B., Jones, K.W., and Adler, P.M., 1994, Synchrotron computed microtomography of porous media: Topology and transports: Physical Review Letters, v. 73, p. 2001–2004.

Tait, S., and Jaupart, C., 1992, Compositional convection in a reactive crystalline mush and melt differentiation: Journal of Geophysical Research, v. 97, p. 6735–6756.

Thovert, J.F., Salles, J., and Adler, P.M., 1993, Computerized characterization of the geometry of real porous media: Their discretization, analysis and interpretation: Journal of Microscopy, v. 170, p. 65–79.

von Bargen, N., and Waff, H.S., 1986, Permeabilities, interfacial areas and curvatures of partially molten systems: Results of numerical computations of equilibrium microstructures: Journal of Geophysical Research, v. 91, p. 9261–9276.

Waff, H.S., and Faul, U.H., 1992, Effects of crystalline anisotropy on fluid distribution in ultramafic partial melts: Journal of Geophysical Research, v. 97, p. 9003–9014.

Walte, N.P., Bons, P.D., Passchier, C.W., and Koehn, D., 2003, Disequilibrium melt distribution during static recrystallization: Geology, v. 31, p. 1009–1012.

Wark, D.A., and Watson, E.B., 1998, Grain-scale permeabilities of texturally equilibrated, monomineralic rocks: Earth and Planetary Science Letters, v. 164, p. 591–605.

Wark, D.A., Williams, C.A., Watson, E.B., and Price, J.D., 2003, Reassessment of pore shapes in microstructurally equilibrated rocks, with implications for permeability of the upper mantle: Journal of Geophysical Research, v. 108, no. B1, 2050, doi: 10.1029/2001JB001575.

Watson, E.B., 1982, Melt infiltration and magma evolution: Geology, v. 10, p. 236–240.

Manuscript received 26 January 2004
Revised manuscript received 17 May 2004
Manuscript accepted 18 May 2004

Printed in USA